RESEARCH ARTICLE

Short-term refractive and corneal astigmatism after canal-based microinvasive glaucoma surgery

Colya N. Englisch[1,2*], **Karl T. Boden**[1,3], **André Messias**[1], **Philipp K. Roberts**[1], **André M. Trouvain**[1], **Peter Szurman**[1,3], **Achim Langenbucher**[2], **Philip Wakili**[1*]

1 Eye Clinic Sulzbach, Knappschaft Hospitals Saar, Sulzbach/Saar, Germany, **2** Department of Experimental Ophthalmology, Saarland University, Homburg/Saar, Germany, **3** Klaus Heimann Eye Research Institute (KHERI), Sulzbach/Saar, Germany

* colya.englisch@uni-saarland.de (CNE); Philip.Wakili@Knappschaft-Kliniken.de (PW)

OPEN ACCESS

Citation: Englisch CN, Boden KT, Messias A, Roberts PK, Trouvain AM, Szurman P, et al. (2026) Short-term refractive and corneal astigmatism after canal-based microinvasive glaucoma surgery. PLoS One 21(1): e0340377. https://doi.org/10.1371/journal.pone.0340377

Editor: Nader Hussien Lotfy Bayoumi, Alexandria University Faculty of Medicine, EGYPT

Received: May 28, 2025

Accepted: December 20, 2025

Published: January 8, 2026

Data availability statement: All relevant data are within the manuscript and its Supporting Information files.

Funding: The author(s) received no specific funding for this work.

Abstract

Purpose

To investigate changes in refractive and corneal astigmatism after Hydrus Microstent (Alcon Inc., Geneva, Switzerland) implantation during microinvasive glaucoma surgery.

Setting

One German medical center.

Design

Retrospective, non-randomized, observational cohort study.

Methods

Subjective refraction was obtained mandatorily and keratometry (Pentacam, OCULUS Optikgeräte GmbH, Wetzlar, Germany) optionally preoperatively and after 3 months (D90). Refractive astigmatism was analyzed using three-dimensional (3D) power vectors, including the spherical equivalent, M, the Jackson cross-cylinder projections to the 0° and 90° meridian (J_0) and to the 45° and 135° meridian (J_{45}), and the blurring power vector B. Corneal anterior and posterior surface astigmatism was investigated using the vectorial parameters J_0, J_{45}, and B. A 3D power vector time-course analysis of refractive astigmatism was performed using multivariate pairwise testing, and linear mixed-effects models, accounting for patient ID as a random effect, were used for the remaining analyses.

Competing interests: The authors have declared that no competing interests exist.

Results

A total of 90 ocular hypertension/glaucoma eyes were included. Sixty eyes were implanted with a Hydrus Microstent and phacoemulsified, and 30 eyes underwent implantation as a stand-alone procedure. Univariate analysis of the refractive cylinder showed no variation over time in any cohort (Phacoemulsification: C_{D0} = –1.3 ± 0.9 D vs. C_{D90} = –1.2 ± 1.2 D, P = 0.6; Stand-alone: C_{D0} = –1.6 ± 1.3 D vs. C_{D90} = –1.6 ± 1.2 D, P = 0.9), and no relevant time–by–group interaction was observed. Multivariate astigmatism analysis (M, J_0, J_{45}) indicated a significant change in the phacoemulsification cohort (P = 0.0003), in contrast to the stand-alone procedure cohort (P = 0.5). In the phacoemulsification cohort, B significantly declined from 2.9 ± 2.8 D to 1.2 ± 1.0 D (P < 0.0001) but remained stable in the stand-alone group (2.7 ± 3.5 D to 2.8 ± 3.4 D, P = 0.07). Corneal astigmatism analysis, based on 55 eyes from 37 patients, showed that the magnitudes of the J_0 and J_{45} vectors remained stable over time for both the anterior (D0: J_0 = –0.12 ± 0.07 D, D90: J_0 = –0.21 ± 0.07 D, P = 0.12; D0: J_{45} = –0.05 ± 0.05 D, D90: J_{45} = –0.01 ± 0.05 D, P = 0.5) and posterior surfaces (D0: J_0 = 0.12 ± 0.01 D, D90: J_0 = 0.13 ± 0.01 D, P = 0.3; D0: J_{45} = –0.01 ± 0.01 D, D90: J_{45} = –0.01 ± 0.01 D; P = 0.9), without significant effects of time, group, or their interaction.

Conclusions

The Hydrus Microstent is neutral in refractive astigmatism when used as a stand-alone procedure. In contrast, combined implantation with phacoemulsification can induce changes in refractive astigmatism. Keratometry analysis confirmed that both anterior and posterior corneal astigmatism remain stable, indicating that refractive changes are likely due to internal factors associated with lens exchange rather than the stent itself. Therefore, when implanted alone, the Hydrus Microstent is unlikely to compromise the results of prior refractive treatments.

Introduction

Despite considerable efforts, glaucoma remains one of the most common causes of irreversible blindness worldwide [1]. Intraocular pressure (IOP) is recognized as the most important modifiable risk factor in glaucoma, and glaucoma treatment relies primarily on medical and surgical strategies to reduce and stabilize IOP [2]. Microinvasive glaucoma surgery (MIGS) includes devices that are designed to shunt aqueous outflow into Schlemm's canal, the suprachoroidal or subconjunctival space [3–5]. In primary open-angle glaucoma eyes, aqueous outflow obstruction presumably relies on resistance-increasing trabecular meshwork alteration [2,6]. The Hydrus Microstent (Alcon Inc., Geneva, Switzerland) is precisely designed for implantation into Schlemm's canal, thus creating direct access to the canal and increasing the outflow facility of the trabecular meshwork in this quadrant [7,8]. Recent research has shown that the Hydrus Microstent is safe and can substantially reduce outflow resistance and stabilize IOP [9,10].

Of note, the nasal and inferior quadrants of the trabecular meshwork have the highest density of collector channels associated with areas of active outflow [11]. Therefore, the Hydrus Microstent is most commonly implanted in these quadrants, as it maximizes the number of collector channels accessed beyond Schlemm's canal. Implantation can be performed in combination with cataract surgery [12,13] or as stand-alone procedure [14].

Previous histological and scanning electron microscopy studies in non-human primates displayed no evidence of inflammation, granulation, or fibrosis in the aqueous outflow system or in surrounding tissues [15].

Nevertheless, the close proximity to inner corneal layers could allow the Hydrus Microstent to alter the corneal keratometry, for example, through extracellular matrix reduction, focal corneal oedema, or mechanical irritation of the chamber angle architecture, and ultimately to induce refractive changes.

Furthermore, the Hydrus Microstent is composed of nitinol, a shape-memory material. After implantation, it returns to its original shape and curvature. Notably, the asymmetrical force exerted by the quadrant-specific implantation on the surrounding structures could create local micromechanical tensions and deformations, ultimately leading to irregular shifts of the corneal curvature. As a consequence, irregular astigmatism components, as well as axis deviations, are conceivable, which are trackable using enhanced methods such as three-dimensional (3D) power-vector analysis. The aim of this study was to investigate the impact of Hydrus Microstent implantation on the occurrence or development of postoperative refractive and corneal astigmatism using a vector analysis.

Methods

Study design

This retrospective, non-randomized, uncontrolled, observational cohort study aimed to assess the short-term refractive and corneal astigmatism in glaucoma or ocular hypertension patients receiving Hydrus Microstent implantation as a stand-alone procedure or combined with phacoemulsification. Ophthalmological examination was scheduled preoperatively at baseline or day 0 (D0) and 90 days postoperatively (D90) and included slit-lamp microscopy, dilated fundus examination, Goldmann applanation tonometry, subjective refraction (sphere, cylinder, and axis), and corrected-distance visual acuity (CDVA, in LogMAR units [logarithm of the minimum angle of resolution]). Keratometry was not a prerequisite for study inclusion and was only analysed when available directly preoperatively and at D90 (Pentacam, OCULUS Optikgeräte GmbH, Wetzlar, Germany).

Exclusion criteria included myopia of more than –6 diopters (D), hyperopia of more than +4 D, an axial length shorter than 22 and longer than 26 mm, a sulcus- or scleral-fixated IOL implantation, and eye surgery within 6 months or cataract surgery within 3 months prior to implantation of the Hydrus Microstent. Patients with a CDVA of 0.6 LogMAR or worse, as well as patients with serious general diseases, were also excluded.

Written informed consent was obtained. The study adhered to the tenets of the Declaration of Helsinki and was approved by the local Institutional Review Board (16/17, Ethikkommission bei der Ärztekammer des Saarlandes). For research purposes, data were accessed on December 15th, 2024, June 30th, 2025, and November 15th, 2025. The authors had access to information that could identify individual participants during or after data collection.

Hydrus microstent

The Hydrus Microstent is designed to bypass the trabecular meshwork while dilating roughly 3 clock hours of Schlemm's canal. Full details of the Hydrus Microstent have been reported previously [10]. The long-term biocompatibility of this nitinol-based aqueous drainage device has been demonstrated [15]. Its curvature matches that of Schlemm's canal.

The surgeon introduces the device via the trabecular meshwork, whereby the inlet segment is placed within the anterior chamber. The remaining scaffolding segments are located within 3 clock hours or a quadrant of Schlemm's canal, aiming to impact the draining area of several collector vessels [16].

In 2011, the Hydrus Microstent received Conformité Européenne approval as both a stand-alone procedure and combined with phacoemulsification/cataract surgery.

Surgical technique

The Hydrus Microstent is intended for *ab interno* implantation through the trabecular meshwork into Schlemm's canal, as described in detail by Samuelson *et al*. [10] and Pfeiffer *et al*. [13]. All Hydrus Microstent implantation procedures were carried out by four surgeons with substantial experience in this technique. Correct positioning, defined as full placement of the stent within the Schlemm's canal except for the inlet aperture, was assessed intraoperatively using a Swan-Jacobs gonioprism.

For the stand-alone procedure, two 1.2 mm wide clear-cornea side-port incisions were created. When combined with phacoemulsification, an additional temporal 2.4 mm clear-cornea main incision was created. The SENSAR™ Monofocal 1-Piece IOL (Johnson & Johnson) was implanted in all patients undergoing the combined procedure.

Power vector analysis

Refractive astigmatism was displayed using a 3D power-vector system. As recommended by Thibos and Horner [17], we used three vector components: 1st, M, the spherical equivalent; 2nd, J_0, the Jackson cross-cylinder C projection to the 0° and 90° meridian; and 3rd, J_{45}, the C projection to the 45° and 135° meridian. The following formulae were used for calculation, where S is the sphere (D), C is the cylinder (D), and α is the axis (°).

$$M = \mathrm{S} + \mathrm{C}/2$$

$$J_0 = (-\mathrm{C}/2)\cos(2\alpha)$$

$$J_{45} = (-\mathrm{C}/2)\sin(2\alpha)$$

To determine the impact of surgery on astigmatism, we also calculated the blurring power vector, B [17]. B_{change} represents the change in B between two time points.

$$B = \sqrt{M^2 + {J_0}^2 + {J_{45}}^2}$$

$$B_{change} = \sqrt{(M - M')^2 + (J_0 - J_0')^2 + (J_{45} - J_{45}')^2}$$

Keratometry-derived corneal anterior and posterior surface astigmatism analysis was performed using the vectorial parameters J_0, J_{45}, and B, calculated as follows:

$$B = \sqrt{{J_0}^2 + {J_{45}}^2}$$

Statistical analysis

The Shapiro–Wilk test was used to assess normality of univariate datasets. Quantitative and qualitative baseline characteristics of the phacoemulsification and stand-alone procedure cohorts were compared using the Mann–Whitney U test and Fisher's exact test, respectively. The Wilcoxon signed-rank test was used to detect time course in CDVA.

Multivariate power-vector analysis of refractive astigmatism involved the three power-vector components: M, J_0, and J_{45}. Henze-Zirkler's and Royston's methods were used to test normality for multivariate datasets. The nonparametric rank-sum test was used for time course analysis of the paired datasets.

Because both eyes from the same patient could be included, and repeated measurements were available over time (D0 and D90), we accounted for within-subject correlation using linear mixed-effects models (LMM) for both refractive and keratometry-derived corneal anterior and posterior surface astigmatism analysis. Patient identification number (ID) and surgeon identity were included as random effects, whereas time and/or surgical group was included as a fixed effect. Intraoperative complications were incorporated as an additional variable. Multivariate linear mixed-effects regression (MLR) was used to investigate the influence of age, sex, M_{D0}, and IOP on B_{Change}, with patient ID included as a random effect.

A post hoc power analysis was conducted using G*Power (version 3.1), applying the "Means – Wilcoxon signed-rank test (matched pairs)" module to assess the statistical power for detecting changes in B over time.

Data are reported as mean ± standard deviation for descriptive purposes. P values were two-sided and considered statistically significant when < 0.05. MATLAB was used for multivariate analysis (version R2023b, MathWorks, Inc). JMP (version 16.2.0, SAS Institute, Inc.) was used for the remaining statistical analyses and for generating double-angle plots.

Results

Subjects

The Hydrus Microstent was successfully implanted in 90 eyes from 74 patients. Thirty eyes underwent stand-alone implantation, while 60 eyes received the stent combined with cataract surgery. Table 1 summarizes the baseline characteristics for all eyes in both cohorts.

The preoperative CDVA was 0.4 ± 0.4, 0.3 ± 0.5, and 0.4 ± 0.4 LogMAR for the total, stand-alone, and phacoemulsification groups, respectively. By postoperative day 90, CDVA improved to 0.2 ± 0.4 in both the total and phacoemulsification cohorts ($P < 0.0001$, Wilcoxon signed-rank test), while remaining unchanged in the stand-alone cohort (0.3 ± 0.5, $P = 0.4$, Wilcoxon signed-rank test).

No major complications occurred. Minor events were infrequent and mild, and are summarized in Table 1. Two cases of postoperative macular edema occurred in the phacoemulsification group.

Spherical equivalent

The spherical equivalent M did not significantly change between baseline and 3 months. In the overall cohort, M_{D0} was –1.5 ± 3.8 D and M_{D90} was –1.1 ± 2.5 D ($P = 0.3$, LMM). Baseline values were similar between the phacoemulsification (M_{D0} = –1.2 ± 3.8 D) and stand-alone groups (M_{D0} = –2.0 ± 3.8 D, $P = 0.1$, LMM), and neither subcohort showed a significant change over time (Phacoemulsification: M_{D90} = –0.6 ± 1.2 D; Stand-alone: M_{D90} = –1.9 ± 3.8 D; both $P > 0.2$, LMM).

Refractive astigmatism

In the total cohort, refractive cylinder did not change over time, measuring –1.4 ± 1.1 D at baseline and –1.3 ± 1.2 D at 3 months ($P = 0.7$, LMM). Baseline values were comparable between the phacoemulsification group (C_{D0} = –1.3 ± 0.9 D) and the stand-alone group (C_{D0} = –1.6 ± 1.3 D, $P = 0.2$, LMM). Neither group showed a significant change in refractive cylinder over time (Phacoemulsification: C_{D90} = –1.2 ± 1.2 D, $P = 0.6$, LMM; Stand-alone: C_{D90} = –1.6 ± 1.2 D, $P = 0.9$, LMM), and no relevant time–by–group interaction was observed.

Fig 1 displays double-angle plots showing refractive astigmatism at baseline and D90.

In the phacoemulsification cohort, multivariate power-vector analysis (M, J_0, J_{45}) demonstrated a significant shift in refractive astigmatism over time ($P = 0.0003$, rank-sum test), whereas no significant change was observed in the stand-alone procedure cohort ($P = 0.5$, rank-sum test).

Table 1. Distribution of patient characteristics receiving the Hydrus Microstent in combination with phacoemulsification or undergoing implantation as a stand-alone procedure.

	Total Cohort	Phacoemulsification Cohort	Stand-alone Procedure Cohort	*P*-value
Total				
Eyes	90	60	30	
Patients	74	48	26	
Sex				
Male	34	23	11	0.5#
Female	40	25	15	
Age (years)	70.0 ± 10.3	68.7 ± 7.4	72.2 ± 14.1	0.03*
Eye				
Right	45	30	15	0.9#
Left	45	30	15	
Intraocular Pressure (mmHg)	19.7 ± 7.2	19.3 ± 5.8	20.7 ± 9.6	0.9*
Diagnosis				
Chronic Primary Open-Angle Glaucoma	47	31	16	0.06#
Normal Tension Glaucoma	7	6	1	
Pseudoexfoliative Glaucoma	17	11	6	
Pigmentary Glaucoma	6	5	1	
Uveitic Glaucoma	1	1	0	
Rubeotic Glaucoma	0	0	0	
Aphakia Glaucoma	0	0	0	
Juvenile Glaucoma	0	0	0	
Angle Closure Glaucoma	3	3	0	
Traumatic Glaucoma	1	0	1	
Ocular Hypertension	8	3	5	
Previous Glaucoma Surgery				
Trabeculectomy	1	0	1	0.6#
Trabeculotomy	1	1	0	
Canaloplasty	2	1	1	
Lens Status				
Phakia	69	60	9	< 0.0001#
Pseudophakia	21	0	21	
Ocular Comorbidity				
Amblyopia	2	1	1	0.1#
Exudative Age-related Macular	7	4	3	
Degeneration				
Dry Geographical Atrophy	1	1	0	
Diabetic Macular Oedema	0	0	0	
Irvine Gass Oedema	2	1	1	
Epiretinal Gliosis	2	2	0	
Vascular Occlusion	4	2	2	
Lamellar Macular Hole	4	4	0	
Full Thickness Macular Hole	1	1	0	
Anterior Ischemic Neuropathy	1	0	1	
Keratoconus	1	1	0	

(Continued)

Table 1. (Continued)

	Total Cohort	Phacoemulsification Cohort	Stand-alone Procedure Cohort	*P*-value
Intraoperative Complications				
Intracameral Bleeding	19	15	4	<0.0001#
Multiple Implantation Attempts	8	2	6	
Device Repositioning	6	6	0	

Patients' sex and age, laterality (right or left), intraocular pressure, diagnosis, previous glaucoma surgery, lens status, visual acuity reducing ocular comorbidities, and intraoperative complications were recorded. # Fisher's exact test, * Mann–Whitney *U* tests comparing the phacoemulsification with the stand-alone procedure cohort.

https://doi.org/10.1371/journal.pone.0340377.t001

Overall, the average magnitude of the vector *B* was 2.9 ± 3.0 D at baseline and decreased to 1.8 ± 2.3 D at D90 ($P = 0.0003$, LMM). In the phacoemulsification cohort, *B* significantly declined from 2.9 ± 2.8 D to 1.2 ± 1.0 D ($P < 0.0001$, LMM) but remained stable in the stand-alone group (2.7 ± 3.5 D to 2.8 ± 3.4 D, $P = 0.07$, LMM).

The average B_{Change} vector ($M - M'$, $J_0 - J_0'$, $J_{45} - J_{45}'$) was 1.9 ± 2.0 D in the overall cohort and, consistently with the behavior of *B*, was significantly larger in the phacoemulsification group ($B_{Change} = 2.6 \pm 2.2$ D) than in the stand-alone group ($B_{Change} = 0.6 \pm 0.4$ D, $P < 0.0001$ LMM). The MLR identified only M_{D0} as a significant predictor of B_{Change}, with a more myopic M_{D0} being associated with a larger reduction in *B* ($R^2 = 0.16$, $P < 0.0001$), whereas age ($R^2 = 0.009$, $P = 0.4$), sex ($R^2 < 0.001$, $P = 0.9$), and baseline IOP ($R^2 < 0.0001$, $P = 0.9$) showed no influence.

Regarding individual power-vector components, J_0 showed small but significant changes over time and between groups. Overall, J_0 increased slightly from –0.07 ± 0.6 D at D0 to 0.04 ± 0.6 D at D90 ($P = 0.02$, LMM) and was marginally more "with-the-rule" in the stand-alone group than in the phacoemulsification group ($P = 0.04$, LMM). However, the absolute shift magnitude was < 0.2 D and is thus unlikely to be clinically meaningful. No significant effects of time, group, or their interaction were detected for J_{45} ($P > 0.5$, LMM).

Corneal astigmatism

A total of 55 eyes from 37 patients had preoperative and postoperative keratometry data. Twenty eyes from 18 patients, average age 74.1 ± 11.0 years, including 7 men and 11 women, underwent stand-alone implantation. Thirty-five eyes from 29 patients, average age 68.9 ± 7.2 years, including 14 men and 15 women, underwent implantation combined with phacoemulsification.

Anterior surface J_0 remained stable over time in the overall cohort (D0: $J_0 = -0.12 \pm 0.07$ D; D90: $J_0 = -0.21 \pm 0.07$ D, $P = 0.12$, LMM), without significant effects of time, group, or their interaction. Anterior surface J_{45} was close to zero throughout the investigation (D0: $J_{45} = -0.05 \pm 0.05$ D; D90: $J_{45} = -0.01 \pm 0.05$ D, $P = 0.5$, LMM), without significant effects of time, group, or their interaction. The magnitude of anterior surface vector *B* was 1.02 ± 0.10 D at D0 and 1.25 ± 0.10 D at D90. This time course reached statistical significance ($P = 0.007$, LMM), but did not vary between groups at any time point. Fig 2 displays the respective double-angle plots of corneal anterior surface astigmatism.

Posterior surface J_0 was stable near zero both at baseline ($J_0 = 0.12 \pm 0.01$ D) and at 3 months ($J_0 = 0.13 \pm 0.01$ D, $P = 0.3$, LMM), as was J_{45} (D0: $J_{45} = -0.01 \pm 0.01$ D; D90: $J_{45} = -0.01 \pm 0.01$ D; $P = 0.9$, LMM). The magnitude of posterior surface vector *B* was similarly unchanged (D0: $B = 0.29 \pm 0.2$ D; D90: $B = 0.32 \pm 0.02$ D, $P = 0.3$, LMM), without significant effects of time, group, or their interaction.

Impact of intraoperative complications

There was no significant effect of complication type on any postoperative corneal or refractive astigmatism parameter ($P > 0.4$). Least-squares means for all power-vector components were similar across complication categories, with broadly overlapping confidence intervals.

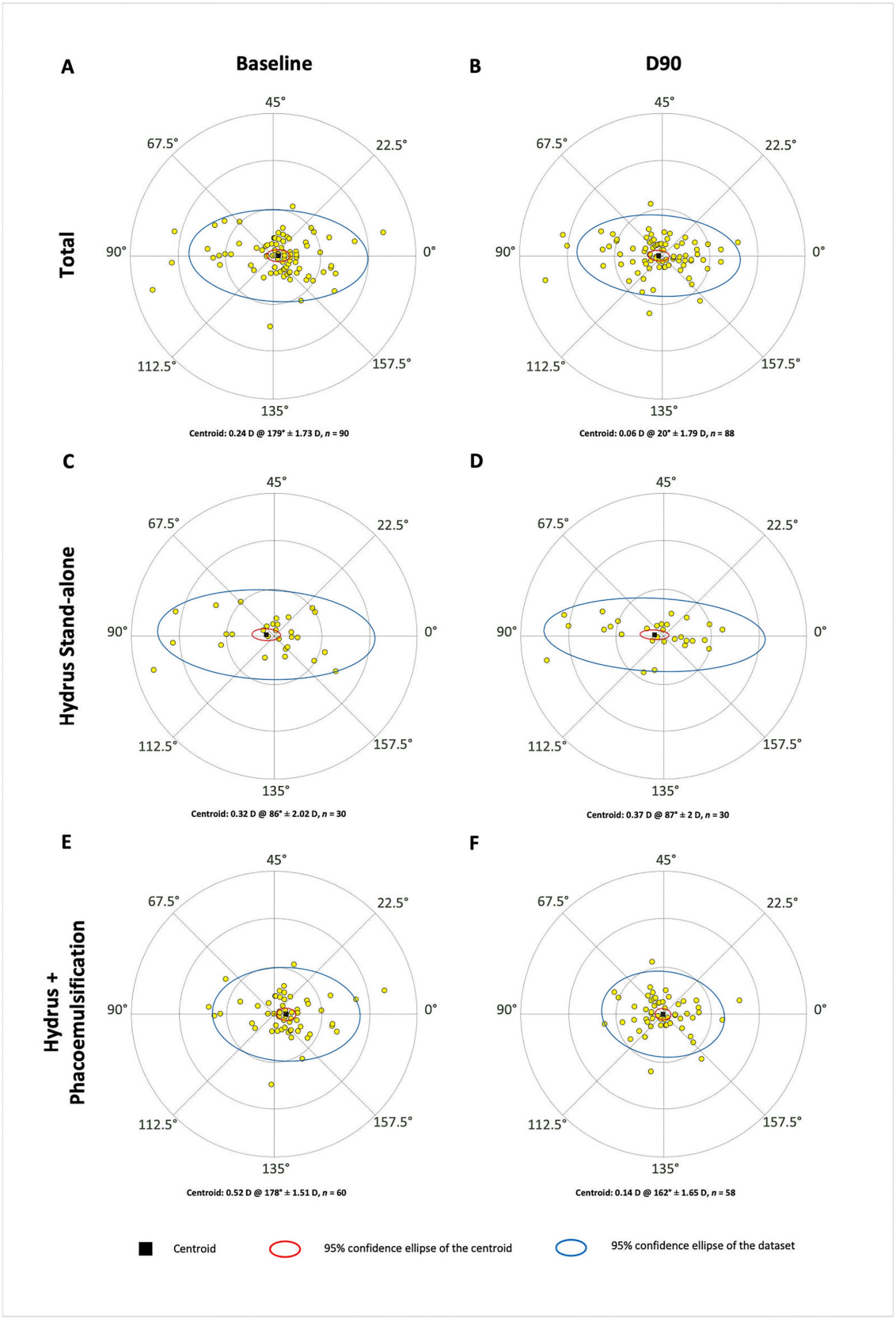
A
Baseline
B
D90
Total
45°
67.5°
22.5°
90°
0°
112.5°
157.5°
135°
Centroid: 0.24 D @ 179° ± 1.73 D, n = 90
Centroid: 0.06 D @ 20° ± 1.79 D, n = 88
C
D
Hydrus Stand-alone
Centroid: 0.32 D @ 86° ± 2.02 D, n = 30
Centroid: 0.37 D @ 87° ± 2 D, n = 30
E
F
Hydrus + Phacoemulsification
Centroid: 0.52 D @ 178° ± 1.51 D, n = 60
Centroid: 0.14 D @ 162° ± 1.65 D, n = 58
Centroid
95% confidence ellipse of the centroid
95% confidence ellipse of the dataset

Fig 1. Double-angle plots illustrating refractive astigmatism at baseline (A, C, and E) and 90 days postoperatively (B, D, and F) for all eyes (A and B) and both subcohorts separately (*i.e.*, stand-alone [C and D] and phacoemulsification [E and F]). Centroid values (written and graphically represented as black squares), standard deviations, and 95% confidence ellipses for both the centroid (in red) and dataset (in blue) are displayed.

https://doi.org/10.1371/journal.pone.0340377.g001

Post hoc power analysis

A post hoc power analysis based on the total sample size of 90 eyes, an alpha level of 0.05, and an estimated effect size (dz) of approximately 0.4 yielded a statistical power of 0.96 for detecting changes in *B* between the two time points.

Discussion

The objective of this retrospective, non-randomized, uncontrolled, observational cohort study was to evaluate short-term postoperative astigmatism following stand-alone Hydrus Microstent implantation and in combination with phacoemulsification. Although prior studies have investigated the performance and safety of the Hydrus Microstent [9,10,13], detailed astigmatism analyses have not been conducted. However, this is particularly important because astigmatism changes resulting from Schlemm's canal interventions can impact visual acuity and ultimately affect the patient satisfaction and quality of life.

Subconjunctival MIGS, such as XEN GelStent and Preserflo Microshunt, as well as ab interno trabecular procedures like microhook trabeculotomy, have been shown to have minimal impact on astigmatism [18,19]. Nonpenetrating glaucoma surgery, such as canaloplasty, can induce transient postoperative astigmatism that typically returns to baseline within six months [20,21], while even suprachoroidal telemetric devices for long-term IOP monitoring are astigmatism-neutral [20,22–24]. However, nitinol, the shape-memory material comprising the Hydrus Microstent, does not adapt to individual anterior segment anatomy, potentially affecting the curvature of the surrounding layers and ultimately inducing astigmatism.

Multivariate 3D power-vector analysis (M, J_0, J_{45}), which provides a robust assessment of astigmatic changes, showed no significant variation between baseline and D90 in the stand-alone cohort, with the B_{Change} vector averaging only 0.6 ± 0.4 D. In contrast, the phacoemulsification cohort demonstrated a significant time course, with a B_{Change} vector of 2.6 ± 2.2 D.

Surgically induced astigmatism is influenced by incision length, type, location, and particularly incision width [25,26]. The 2.4 mm main incision used in phacoemulsification may therefore have contributed to the observed refractive changes, whereas the 1.2 mm side-port incisions are considered astigmatism-neutral [27,28]. Clear corneal incision placement and subsequent wound healing can both influence postoperative astigmatism [29]. Notably, surgically induced astigmatism typically decreases within the first postoperative month, which supports the timeline chosen in this study [27,28]. Despite these considerations, keratometry analysis confirmed complete stability of both anterior and posterior corneal astigmatism components J_0 and J_{45}. The small, though significant, variations observed in the anterior surface vector B likely reflect the inherent variability of measuring low-magnitude corneal astigmatism, influenced by slight alterations in tear film, ring reflections, axis determination, or even minor decentrations, rather than structural changes. Although these keratometry-specific results are derived from a limited sample and warrant confirmation in larger prospective studies, they suggest that the Hydrus Microstent does not induce systematic corneal alterations, and that refractive changes after combined surgery are primarily attributable to internal optical factors related to lens extraction and IOL implantation, such as spherical power shifts or lens tilt.

Inclusion of the variable "intraoperative complications" in LMMs revealed no significant association with any refractive or keratometric parameters, indicating that mild intraoperative events such as intracameral bleeding, multiple implantation attempts, or device repositioning did not measurably affect refractive stability at three months postoperatively.

Notably, age, sex, and baseline IOP had no impact on refractive B_{Change}. Baseline spherical equivalent, M_{D0}, showed an association, but this was expected given its inclusion in the B_{Change} vector calculation. Therefore, no adjustment was made in the main analysis.

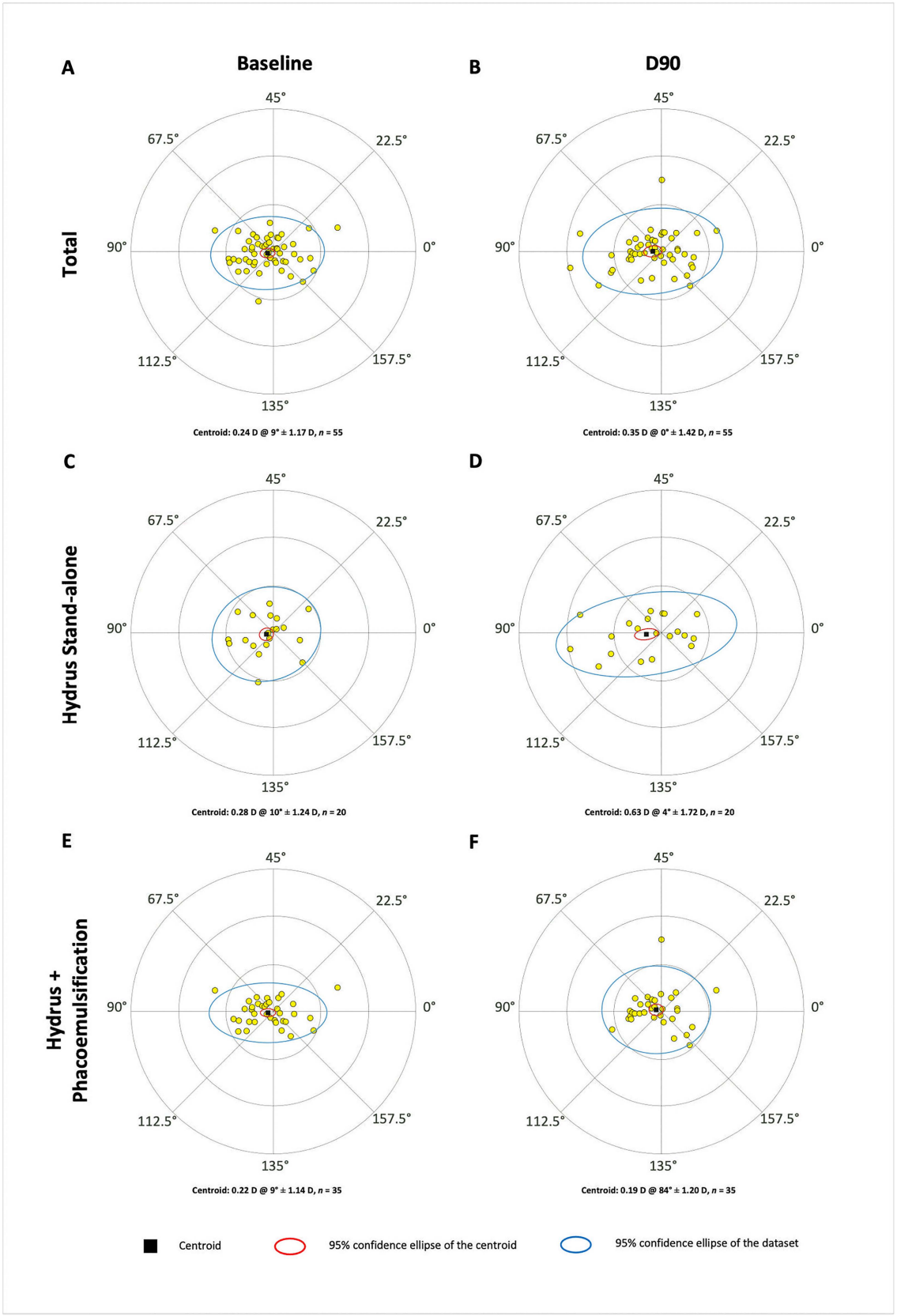
A
Baseline
B
D90
Total
45°
67.5°
22.5°
90°
0°
112.5°
157.5°
135°
Centroid: 0.24 D @ 9° ± 1.17 D, n = 55
Centroid: 0.35 D @ 0° ± 1.42 D, n = 55
C
D
Hydrus Stand-alone
Centroid: 0.28 D @ 10° ± 1.24 D, n = 20
Centroid: 0.63 D @ 4° ± 1.72 D, n = 20
E
F
Hydrus + Phacoemulsification
Centroid: 0.22 D @ 9° ± 1.14 D, n = 35
Centroid: 0.19 D @ 84° ± 1.20 D, n = 35
Centroid
95% confidence ellipse of the centroid
95% confidence ellipse of the dataset

Fig 2. Double-angle plots illustrating anterior surface corneal astigmatism at baseline (A, C, and E) and 90 days postoperatively (B, D, and F) for all eyes (A and B) and both subcohorts separately (*i.e.*, stand-alone [C and D] and phacoemulsification [E and F]). Centroid values (written and graphically represented as black squares), standard deviations, and 95% confidence ellipses for both the centroid (in red) and dataset (in blue) are displayed.

https://doi.org/10.1371/journal.pone.0340377.g002

These findings are important, as they show that Hydrus Microstent implantation—an emerging MIGS procedure with good performance—is astigmatism-neutral in the short-term. However, the study did not assess potential very early, transient shifts occurring within days to weeks, as have been reported with canaloplasty [20,21], which represents a notable limitation. Additional limitations include the retrospective design, a limited sample size, inclusion of several surgeons, and lack of long-term follow-up. However, post hoc power analysis indicated a power greater than 0.9, confirming statistical robustness, and surgeon identity did not significantly influence outcomes. Nevertheless, long-term follow-up is warranted to evaluate a potential sustained or late impact of Hydrus Microstent implantation on corneal and refractive astigmatism.

In conclusion, the Hydrus Microstent is neutral in refractive astigmatism when used as a stand-alone procedure. In contrast, when combined with phacoemulsification, shifts in refractive astigmatism may occur. Keratometry confirmed stable anterior and posterior corneal astigmatism, indicating that these changes are most likely related to internal optical factors of lens exchange. Thus, when implanted alone, the Hydrus Microstent is unlikely to compromise the outcomes of previous refractive treatments.

Supporting information

S1 Table. Raw subjective refraction data at baseline and at 3 months (D90).
(PDF)

Acknowledgments

We wish to thank Kathi Savioli for kindly supporting the data collection and Jenna Flogeras for professional language editing.

Author contributions

Conceptualization: Colya N. Englisch, Karl T. Boden, Philip Wakili.

Data curation: Colya N. Englisch.

Formal analysis: Colya N. Englisch, André Messias.

Investigation: Colya N. Englisch, Philipp K. Roberts, André M. Trouvain, Peter Szurman, Achim Langenbucher, Philip Wakili.

Methodology: Colya N. Englisch, André Messias, Achim Langenbucher.

Resources: Peter Szurman.

Writing – original draft: Colya N. Englisch.

Writing – review & editing: Colya N. Englisch, Karl T. Boden, André Messias, Philipp K. Roberts, André M. Trouvain, Peter Szurman, Achim Langenbucher, Philip Wakili.

References

1. GBD 2019 Blindness and Vision Impairment Collaborators, Vision Loss Expert Group of the Global Burden of Disease Study. Causes of blindness and vision impairment in 2020 and trends over 30 years, and prevalence of avoidable blindness in relation to VISION 2020: the Right to Sight: an analysis for the Global Burden of Disease Study. Lancet Glob Health. 2021;9(2):e144–60. https://doi.org/10.1016/S2214-109X(20)30489-7 PMID: 33275949

2. Weinreb RN, Leung CKS, Crowston JG, Medeiros FA, Friedman DS, Wiggs JL, et al. Primary open-angle glaucoma. Nat Rev Dis Primers. 2016;2:16067. https://doi.org/10.1038/nrdp.2016.67 PMID: 27654570
3. Chan PPM, Larson MD, Dickerson JE Jr, Mercieca K, Koh VTC, Lim R, et al. Minimally Invasive Glaucoma Surgery: Latest Developments and Future Challenges. Asia Pac J Ophthalmol (Phila). 2023;12(6):537–64. https://doi.org/10.1097/APO.0000000000000646 PMID: 38079242
4. Lim R. The surgical management of glaucoma: A review. Clin Exp Ophthalmol. 2022;50(2):213–31. https://doi.org/10.1111/ceo.14028 PMID: 35037376
5. Nichani P, Popovic MM, Schlenker MB, Park J, Ahmed IIK. Microinvasive glaucoma surgery: A review of 3476 eyes. Surv Ophthalmol. 2021;66(5):714–42. https://doi.org/10.1016/j.survophthal.2020.09.005 PMID: 32998003
6. Tamm ER, Braunger BM, Fuchshofer R. Intraocular Pressure and the Mechanisms Involved in Resistance of the Aqueous Humor Flow in the Trabecular Meshwork Outflow Pathways. Prog Mol Biol Transl Sci. 2015;134:301–14. https://doi.org/10.1016/bs.pmbts.2015.06.007 PMID: 26310162
7. Gulati V, Fan S, Hays CL, Samuelson TW, Ahmed IIK, Toris CB. A novel 8-mm Schlemm's canal scaffold reduces outflow resistance in a human anterior segment perfusion model. Invest Ophthalmol Vis Sci. 2013;54(3):1698–704. https://doi.org/10.1167/iovs.12-11373 PMID: 23372057
8. Camras LJ, Yuan F, Fan S, Samuelson TW, Ahmed IK, Schieber AT, et al. A novel Schlemm's Canal scaffold increases outflow facility in a human anterior segment perfusion model. Invest Ophthalmol Vis Sci. 2012;53(10):6115–21. https://doi.org/10.1167/iovs.12-9570 PMID: 22893672
9. Ahmed IIK, Fea A, Au L, Ang RE, Harasymowycz P, Jampel HD, et al. A Prospective Randomized Trial Comparing Hydrus and iStent Microinvasive Glaucoma Surgery Implants for Standalone Treatment of Open-Angle Glaucoma: The COMPARE Study. Ophthalmology. 2020;127(1):52–61. https://doi.org/10.1016/j.ophtha.2019.04.034 PMID: 31034856
10. Samuelson TW, Chang DF, Marquis R, Flowers B, Lim KS, Ahmed IIK, et al. A Schlemm Canal Microstent for Intraocular Pressure Reduction in Primary Open-Angle Glaucoma and Cataract: The HORIZON Study. Ophthalmology. 2019;126(1):29–37. https://doi.org/10.1016/j.ophtha.2018.05.012 PMID: 29945799
11. Cha EDK, Xu J, Gong L, Gong H. Variations in active outflow along the trabecular outflow pathway. Exp Eye Res. 2016;146:354–60. https://doi.org/10.1016/j.exer.2016.01.008 PMID: 26775054
12. Fea AM, Rekas M, Au L. Evaluation of a Schlemm canal scaffold microstent combined with phacoemulsification in routine clinical practice: Two-year multicenter study. J Cataract Refract Surg. 2017;43(7):886–91. https://doi.org/10.1016/j.jcrs.2017.04.039 PMID: 28823433
13. Pfeiffer N, Garcia-Feijoo J, Martinez-de-la-Casa JM, Larrosa JM, Fea A, Lemij H, et al. A Randomized Trial of a Schlemm's Canal Microstent with Phacoemulsification for Reducing Intraocular Pressure in Open-Angle Glaucoma. Ophthalmology. 2015;122(7):1283–93. https://doi.org/10.1016/j.ophtha.2015.03.031 PMID: 25972254
14. Fea AM, Ahmed IIK, Lavia C, Mittica P, Consolandi G, Motolese I, et al. Hydrus microstent compared to selective laser trabeculoplasty in primary open angle glaucoma: one year results. Clin Exp Ophthalmol. 2017;45(2):120–7. https://doi.org/10.1111/ceo.12805 PMID: 27449488
15. Grierson I, Saheb H, Kahook MY, Johnstone MA, Ahmed IIK, Schieber AT, et al. A Novel Schlemm's Canal Scaffold: Histologic Observations. J Glaucoma. 2015;24(6):460–8. https://doi.org/10.1097/IJG.0000000000000012 PMID: 24240886
16. Johnstone MA, Saheb H, Ahmed IIK, Samuelson TW, Schieber AT, Toris CB. Effects of a Schlemm canal scaffold on collector channel ostia in human anterior segments. Exp Eye Res. 2014;119:70–6. https://doi.org/10.1016/j.exer.2013.12.011 PMID: 24374259
17. Thibos LN, Horner D. Power vector analysis of the optical outcome of refractive surgery. J Cataract Refract Surg. 2001;27(1):80–5. https://doi.org/10.1016/s0886-3350(00)00797-5 PMID: 11165859
18. Tanito M, Matsuzaki Y, Ikeda Y, Fujihara E. Comparison of surgically induced astigmatism following different glaucoma operations. Clin Ophthalmol. 2017;11:2113–20. https://doi.org/10.2147/OPTH.S152612 PMID: 29238159
19. Wagner FM, Schuster AK, Munder A, Muehl M, Chronopoulos P, Pfeiffer N, et al. Comparison of subconjunctival microinvasive glaucoma surgery and trabeculectomy. Acta Ophthalmol. 2022;100(5):e1120–6. https://doi.org/10.1111/aos.15042 PMID: 34626093
20. Englisch CN, Boden KT, Szurman P, Mansouri K, Dick HB, Hoffmann EM, et al. Long-term astigmatism after intraocular pressure sensor implantation and nonpenetrating glaucoma surgery: EYEMATE-SC trial. J Cataract Refract Surg. 2024;50(9):899–905. https://doi.org/10.1097/j.jcrs.0000000000001470 PMID: 38662577
21. Moelle MC, Cursiefen C, Rejdak R, Horn FK, Jünemann AGM. Time course of induced astigmatism after canaloplasty. J Glaucoma. 2014;23(1):e53-9. https://doi.org/10.1097/IJG.0b013e31829f9c31 PMID: 24370811
22. Szurman P, Gillmann K, Seuthe A-M, Dick HB, Hoffmann EM, Mermoud A, et al. EYEMATE-SC Trial: Twelve-Month Safety, Performance, and Accuracy of a Suprachoroidal Sensor for Telemetric Measurement of Intraocular Pressure. Ophthalmology. 2023;130(3):304–12. https://doi.org/10.1016/j.ophtha.2022.09.021 PMID: 36202141
23. Szurman P, Mansouri K, Dick HB, Mermoud A, Hoffmann EM, Mackert M, et al. Safety and performance of a suprachoroidal sensor for telemetric measurement of intraocular pressure in the EYEMATE-SC trial. Br J Ophthalmol. 2023;107(4):518–24. https://doi.org/10.1136/bjophthalmol-2021-320023 PMID: 34772665
24. Englisch CN, Trouvain AM, Wakili P, Mansouri K, Burkhard Dick H, Hoffmann EM, et al. Intraocular Pressure Fluctuations Recorded by a Telemetric Sensor after Nonpenetrating Glaucoma Surgery in Primary Open-Angle Glaucoma. Ophthalmol Glaucoma. 2025;S2589-4196(25)00152-8. https://doi.org/10.1016/j.ogla.2025.07.007 PMID: 40714264
25. Ermiş SS, Inan UU, Oztürk F. Surgically induced astigmatism after superotemporal and superonasal clear corneal incisions in phacoemulsification. J Cataract Refract Surg. 2004;30(6):1316–9. https://doi.org/10.1016/j.jcrs.2003.11.034 PMID: 15177610

26. Kohnen T, Dick B, Jacobi KW. Comparison of the induced astigmatism after temporal clear corneal tunnel incisions of different sizes. J Cataract Refract Surg. 1995;21(4):417–24. https://doi.org/10.1016/s0886-3350(13)80532-9 PMID: 8523286

27. Yang J, Wang X, Zhang H, Pang Y, Wei R-H. Clinical evaluation of surgery-induced astigmatism in cataract surgery using 2.2 mm or 1.8 mm clear corneal micro-incisions. Int J Ophthalmol. 2017;10(1):68–71. https://doi.org/10.18240/ijo.2017.01.11 PMID: 28149779

28. Yu Y-B, Zhu Y-N, Wang W, Zhang Y-D, Yu Y-H, Yao K. A comparable study of clinical and optical outcomes after 1.8, 2.0 mm microcoaxial and 3.0 mm coaxial cataract surgery. Int J Ophthalmol. 2016;9(3):399–405. https://doi.org/10.18240/ijo.2016.03.13 PMID: 27158610

29. Ofir S, Abulafia A, Kleinmann G, Reitblat O, Assia EI. Surgically induced astigmatism assessment: comparison between three corneal measuring devices. J Refract Surg. 2015;31(4):244–7. https://doi.org/10.3928/1081597X-20150319-04 PMID: 25884579